Available online at www.sciencedirect.com

ScienceDirect

Procedia Engineering 173 (2017) 331 – 338

Procedia Engineering

www.elsevier.com/locate/procedia

11th International Symposium on Plasticity and Impact Mechanics, Implast 2016

Investigations on Steel Fibre Reinforced Cementitious Composite Panels under High Velocity Impact of Short Projectiles

Amar Prakash[a]*, A. Rama Mohan Rao[b], S. M. Srinivasan[c]

[a, b]*CSIR-Structural Engineering Research Centre, CSIR Campus, Taramani, Chennai-600113, India*
[c]*Department of Applied Mechanics, IIT Madras, Chennai-600036, India*

Abstract

Response of steel fibre reinforced cementitious composite (SFRCC) panels subjected to high velocity impact of short projectiles have great significance in designing protective structures. Numerical investigation carried out to determine the high velocity impact responses of SFRCC (300 mm square) panels is presented. In order to model the high velocity impact behaviour of SFRCC in the post peak region, the constitutive model of Riedel, Hiermaier and Thoma (RHT) is used with suitable modification in damage parameters. The numerical studies presented in this paper are validated using the experimental investigations carried out by the authors. The influences of steel fibrevolumes (0, 2, 4, 6, 8, and 10%) and thickness of panels (50, 60, 75, 100 mm), on depth of penetration (DOP) and crater dimensions is also investigated. Based on the numerical simulations, the important phenomenon like scabbing and perforation in the SFRCC panels are predicted for the chosen in-service ammunition (7.62 mm calibre) and munitions (AK - 47 rifle).

Peer-review under responsibility of the organizing committee of Implast 2016

Keywords: High velocity impact; steel fibre reinforcement; cementitious composites; RHT constitutive model;short projectiles; axi-symmetric model; Lagrangian approach.

* Corresponding author. Tel.: +91-44-22549179; fax: +91-44-22541508.
*E-mail address:*amar@serc.res.in

Peer-review under responsibility of the organizing committee of Implast 2016
doi:10.1016/j.proeng.2016.12.026

1. Introduction

In the real world all the processes are dynamic, however, in some of the processes, the time involved to observe a physical change is so large that we treat them as static (or independent of time) for example creep, shrinkage and quasi-static testing. On the other hand, some process shows very high rate of deformation due to impulsive loading, such as impact and blast [1]. When dynamic loading is applied to a structure, the inertia begins to play a role in the solution process, which is negligible in the case of quasi-static loading. Further, if the rate of loading is very high (More than 10^4 s^{-1}), then shock wave propagation through the materials also governs the response of structures. In many civil engineering applications the cementitious composite as well as concrete structures are subjected to a variety of accidental or intentional impact loads, apart from static loads. Typical examples of such loads are reported in literature[2-5]. From various sources such as terrorist attacks using bombs or rockets; and missiles or airplane collision to important civilian and military buildings; ship collision to offshore platform and into bridge piers; boulder moved by waves hitting flood defenses; natural disasters such as tornados, tsunamis and earthquakes; vehicle crash into concrete barriers; pile driving; columns in underground car parks; overpass bridges and medium to low rise buildings located close to major roads and intersections; rock falls on the roadways in mountain areas.

Among above mentioned sources of impact loading, the short projectile impact on cementitious composite targets, made by means of in-service munitions (or weapons), is specifically investigated through experimental and numerical studies in the present paper and hence the review also limited to it. During high velocity impact of the short projectile on a target very high pressure is developed at the point of contact. Due to the very high magnitude of stresses and pressure developed at the point of impact, the materials, in both the target and projectile undergo variable strain rates.

2. Behaviour of Cementitious Composite Targets Under High Velocity Impact

2.1 Mechanisms of Impact Damage in Cementitious Composite Targets

When a short projectile hits a cementitious target, a high pressure wave (called as shock wave) is generated at the impact location. This shock wave front propagates through the material of the target as a compressive stress wave and reflects back from stress free boundary of the target as a tensile stress wave. The mathematical basis for this change of compressive stress wave into the tensile stress wave due to reflection at the stress free boundary during shock wave propagation, is explained lucidly in literature [1,6] using one dimensional illustrations. High velocity impact damage in cementitious targets [8-10] can be qualitatively divided into three regions as shown in Fig. 1.

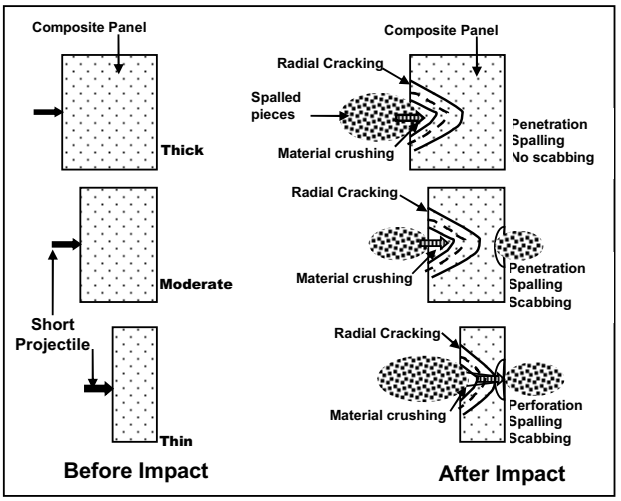

Fig.1 Typical damage in cementitious composite targets of various thickness due to the short projectile impact

These regions are: (i) where the material get crushed due to very high pressure and stresses (ii) where material undergo radial cracking due to stress wave propagation and backward pushing of material (iii) separation of material at the back face due to shock wave reflection at the stress free boundary. The typical damage types in cementitious targets also depend on the thickness of the target with respect to the size of the projectiles. In a thick cementitious composite target the stress magnitude drops to a level lower than the dynamic tensile strength of the material on the back face. This attenuation of stress wave magnitude occurs due to the resistance offered by material damping and inertia. Hence, the scabbing does not occur in thick cementitious composite targets under short projectile impact as shown in Fig.1.

Nonlinear behaviour of cementitious materials, mainly attributed due to meso-mechanical composition of concrete, porous compaction, complex strain localization, micro-cracking, cell wall buckling and plasticity [11]. It is desirable to encompass these micro mechanical effects under a homogenized macro-mechanical description that considers appropriate interdependence between stress, strain, plastic strain, strain rate, damage and failure. A number of constitutive models have been developed to describe cementitious materials like concrete. Few well known models are [12]. Later four models are reviewed and compared in the literature [13]. However, there is no material model available for fiber reinforced composites, which can be used directly in numerical simulations. Recent research [14,15] has proposed certain modifications in the RHT model to capture the post peak behaviour of concrete in a better way as compared to the default parameters given by in-built material library. TheRHT model takes account of pressure hardening, strain hardening, strain rate hardening, third invariant dependence for compressive and tensile meridians, damage effects (strain softening), and crack softening.

It is well established that the rate of increase in uniaxial tensile strength reduces for higher values of compressive strength. In the cases of extreme loading like high velocity impact and blast, the material is subjected to multi-axial stress state, where the lateral stress can reach up to very high magnitude. Due to the high lateral stresses, the confinement occurs which result in an increase of both strength and stiffness. This eventually enhances the ductility.

3. Material Properties

3.1 Materials and mix proportions

The materials used for cementitious composite panels include steel fibres (30 mm long and 0.45 mm in dia), cement OPC 53 grade, fine aggregates (<4.75 mm sieve size, sp. Gr. 2.68, bulk density 1685 kg/m^3, Fineness modulus 2.76), superplasticizers (CONPLAST SP430) etc. Design mix (Cement: sand: W/C: SP) for slurry is taken as 1:1:0.4:0.5% (By weight of cement).

Experimental studies reported in this paper investigate the influence of fiber volume fractions on various mechanical properties of SFRCC. Hence, the fibre volume fractions $v_f$are varied between 0% (No fibre), 2, 4, 6, 8, 10%, while maintaining the same mix proportion of cement-sand slurry in all the specimens. In order to study the effect of thickness of panels various thickness of 300x 300 mm panel namely 50mm, 60mm, 75mm, and 100 mm are considered. The material quantities used for cement, sand slurry as per design mix for one batch of mix, considering the concrete mixer capacity (that is 50 kg load) arecement OPC 53 grade- 20kg; fine sand 20 kg; water 8 kg; and super-plasticizer 100 ml.

3.2 Mixing, casting and curing

Keeping the guidelines of ACI 544 [16] into consideration, the dry cement and fine aggregate are mixed for one minute in a wheel mounted concrete mixer of capacity 50 kg. The mixing is continued for another minute while adding 80% of water. Finally the 100 ml super plasticizer is mixed with remaining 20% of water and it is added to the mix. The mixing is continued for three more minutes to prepare the flowable cement-sand slurry.Fibres weighed as per the volume fractions are placed in specimen moulds in layers alternating with cement sand slurry. It is preferred to use manual compaction as vibrating table is found to be ineffective especially for higher fibre volume fractions. For each fibre volume fraction, six numbers of cylinders of size 100 mm in diameter and 200 mm long, six

numbers of cubes of size 100 mm and 150 mm are prepared for uniaxial compressive strength test, density and sound velocity measurements. For flexure tests prism specimens of size 100 mm x 100 mm x 500 mm for each fibre volume fraction and, for uniaxial tensile strength tests, 25 mm thick standard dogbone specimens are prepared. All the prepared specimens are demoulded after 24 hrs and kept under water in the tank for 28 days of curing. The mechanical properties of SFRCC with respect to fibre content variation as obtained experimentally are furnished in following Table 1.

Table 1- Material properties with varying fibre volume fractions

Percent of fibre	Average density	Ultrasonic Pulse velocity	Modulus of elasticity (Experimental)	Uniaxial tensile strength (ft)	Unconfined compressive strength (fc)
%	Kg/m3	m/s	GPa	MPa	MPa
Plain - 0 %	2265.5	4000.0	31.57	3.14	59.6
SIFCON-2 %	2358.8	4110.1	36.43	5.10	60.2
SIFCON-4 %	2458.5	4130.7	36.56	12.19	74.6
SIFCON-6 %	2568.8	4285.7	37.97	16.11	85.6
SIFCON-8 %	2623.4	4327.1	39.94	17.42	98.4
SIFCON-10 %	2638.4	4137.6	41.55	18.42	106.2
HSC-0%	2450.0	4821.8	43.01	5.00	74.0

4. Numerical Simulation

4.1 The RHT model

The RHT (Riedel, Hiermaier and Thoma) model for cementitious composite materials is expressed in terms of three stress limit surfaces namely, initial yield surface, failure surface, and residual friction surface. During impact these surfaces account for reduction in strength along different meridians.The failure surface i.e. the ultimate strength of the fibre reinforced composite material is formed from material parameters including the compressive, tensile and shear strength. When the stress reaches the failure surface, a parameterized damage model governs the evolution of damage driven by plastic strain, which in turn represents the post failure stress limit surface by interpolating between the initial yield surface and the failure surface and residual surface. The RHT concrete model that has the following modelling capabilities associated with brittle material like cementitious materials; like, Pressure hardening, strain hardening, strain rate hardening, third invariant dependence for compressive and tensile meridians, damage effects (strain softening), and crack-Softening.

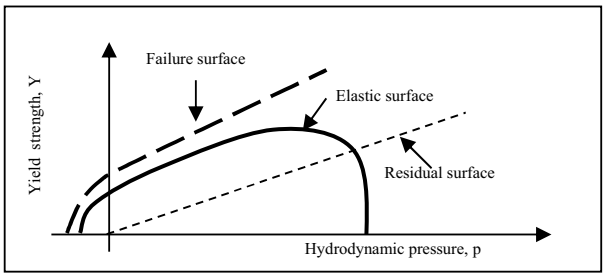

Fig. 2 Typical elastic, failure and residual surfaces of material

For a fully damaged material, there is no meridian or strain rate dependence and shear strength is only supported under confined conditions i.e. positive pressures. This model has been extensively used in literature [17-20]. The recent research [15] is focused on the modification of the input parameters as per the material behaviour.The failure

surface ends this phase and softening phase starts. In this phase the pressure and the stress starts to descend towards the residual surface. If the pressure is applied, with a lower angle, line two (still linear), higher elastic and failure limit is reached as shown in Fig. 2.

4.2 Damage Accumulation in Fibre Reinforced Cementitious Composites

Once cementitious material begins to harden or soften the damage factor D is used to determine the value of the current strength surface. The value of D lies between 0 and 1, which indicate two extremes that is no damage of material and fully damaged material in tension respectively. The damage factor is defined using Equation (1):

$$D = \sum \frac{\Delta \varepsilon^p}{\varepsilon^f} \tag{1}$$

Where, $\Delta \varepsilon^p$ is the accumulated plastic strain and, ε^f is the failure strain given by following Equation (2).

$$\varepsilon^f = D_1 \left(\frac{p}{f_c'} - \frac{p_{spal}}{f_c'} \right)^{D_2} \tag{2}$$

D_1 and D_2 are user input material constants. The default values for D_1 and D_2 are given as 0.04 and 1.0 respectively. Damage causes a reduction in strength. Hence, the strength is modified by shifting the surface from an initial surface to a current damaged one. During softening it is interpolated between the limit and residual surfaces as in Equation (3):

$$Y^* = (1 - D) Y^*_{fail} + D Y^*_{residual} \tag{3}$$

Where,

$$Y^*_{residual} = B * \left(\frac{p}{f_c'} \right)^M \text{ x } [\text{sgn } (\frac{p}{f_c'}) \text{ -1}]/2 \tag{4}$$

In equation (4), the constant B is initial slope of residual surface and, M is residual strength exponent and sgn $(\frac{p}{f_c'})$ is having values 1, 0, -1 for $\frac{p}{f_c'}$ values, greater than 0, equal to 0, and less than 0 respectively. It means that for negative pressure, the residual deviatoric strength vanishes upon total failure; but if confining pressure exists, the material retains a certain level of shear strength due to friction among crushed particle.

4.2.1 Modification proposed to RHT model

Since RHT model is developed primarily to simulate the behaviour of plain concrete, and, hence default values given with respect to plain concrete may not provide satisfactory behaviour for fibre reinforced composites. In view of this suitable modifications are incorporated in RHT model in order to simulate the behaviour of steel fibre reinforced cementitious composite material. Basically, the inclusion of fibres to cementitious concrete or matrix results in improved post-cracking behaviour. Therefore, the main difference between material models used for plain concrete and steel fibre reinforced composite material is the failure description under tension [13-14, 19]. Due to the enhanced ductility of fibre reinforced materials, the crack control ability and energy absorption capacity increases which result in increased impact resistance. Apart from using the experimentally obtained compressive, tensile and shear strength values, the failure strain ε^f is also increased accordingly to match numerical responses with experimental investigations. Due to this increase in failure strain, the value of damage D gets reduced as can be realized from equation (1). Hence, keeping D_2 as constant, the critical value of D_1 parameter in equation (2) is obtained by conducting a separate parametric study on D_1 between 0.02 and 0.1, it is found that the value of 0.06 shows impact responses of SFRCC panels (having fiber volume more than or equal to 4%) closer to the experimental results. Hence for the fibre contents above 4% the value of coefficient D_1 is proposed as 0.06 instead of default 0.04 in AUTODYN [21], material library.

4.3 Computation Using Explicit Time Integration

In this paper the explicit integration is used in the Lagrangian code. When explicit integration schemes are employed to advance solutions in time and the mass matrix is symmetric (this occurs when mass is lumped at the nodes in place of using a distributed mass for an element), then the global stiffness matrix can be bypassed and the integration performed on an element-by-element basis. This results in a very efficient scheme, which does not require evaluation or updating of the global stiffness matrix. The problem of large distortions is associated with the Lagrange codes. Erosion is a numerical mechanism for the automatic removal of severely distorted elements during a simulation.

4.4 Finite Element Mesh

Numerical simulations are carried out by using the advanced analysis software AUTODYN [21]. In order to achieve faster speed of simulations the square geometry of SFRCC panels is modelled with two-dimensional axi-symmetric finite elements. First assumption in axi-symmetric analysis made is far off boundary may not influence results, because the plan dimension of panel in transverse direction is three times of its thickness. Second assumption made due to the transverse shock wave speed (i.e. Rayleigh wave speed) is about 1.6 times slower than the compressive wave speed [22-24]. It clearly indicates that the stress free boundaries are farther in transverse direction than in longitudinal direction. Hence the reflected stress wave from straight or curved surface will not make much difference. Although the distribution of fibres is random in layers during casting, yet it is assumed that material properties are uniform about axis of symmetric. It is worth to mention here that the computational complexity of Lagrangian FE model with solid elements is about 15-20 times more than the axi-symmetric elements. To capture the highly stress gradient at the point of impact finer mesh size is used after several mesh convergence studies. Smooth variation of element size is ensured so that the highly distorted zone contains finer elements as shown for a typical analysis case in Fig. 3.

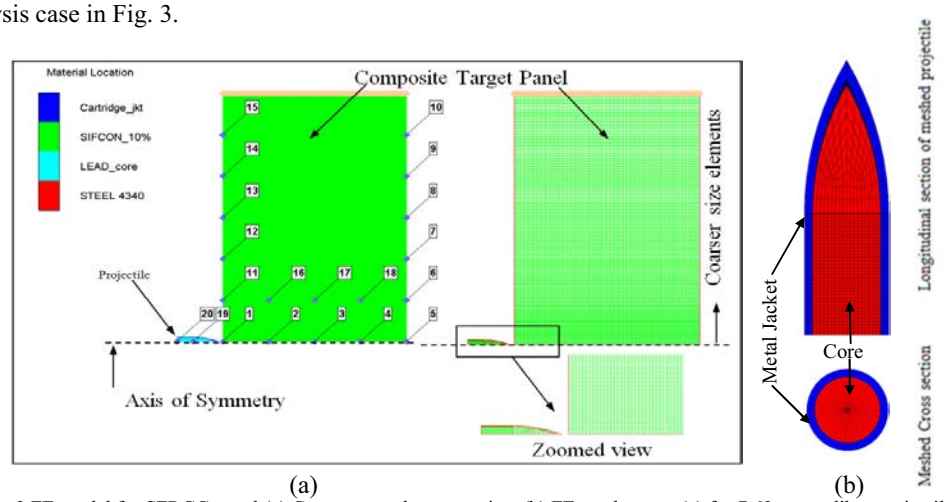

Fig. 3 FE model for SFRCC panel (a) Geometry and gauge points (b) FE mesh target (c) for 7.62 mm calibre projectiles

For 7.62 mm calibre projectile the finite element meshes as used in the present study are shown in Fig. 9(c). The critical gauge points locations defined to capture numerical responses in panel and projectile are (Fig. 9).

4.5 Effect of Thickness of Panel on Impact Performance

In order to understand the behaviour of thickness of SFRCC panel numerical simulation are carried out for various thicknesses like 50 mm, 60 mm, 75 mm, and 100 mm. However, the numerical simulation to determine the thickness effects are restricted to SSS type panels and finally after obtaining the optimum thickness for 10% fibre volume the further simulations are carried out for reduced fibre volume as well which are discussed in next section.

The impact performance of 60 mm and 100 mm thick target panels is shown in Fig. 4. At GP#1 peak pressures recorded in 60 mm and 100 mm thick panels are is 0.935 GPa and 0.8 GPa as shown in Fig. 4. However for 100mm thick panel pressure increases at GP#2, while it is decreasing gradually in 60 mm thick panel.

This very high magnitude of pressure with respect to the compressive strength of target materials causes crushing of the material as well as spalling at the front face. The peak formation indicates the temporal delay during shock wave propagation and interaction. It is also observed that the negative pressure value (27.4 MPa) in 60 mm thick panel at the back face (with respect to GP 5, 6, 7) exceeds uniaxial tensile strength (18.42 MPa) of SIFCON having 10% fibre volume. Hence this difference is responsible for scabbing in thin panels even with high dosage of fibre volumes. On investigating, the SSS type panels with different thickness under both the projectile calibre it is inferred that, if the thickness of SFRCC is about 60±5mm then scabbing is likely to occur as shown in Fig. 5.

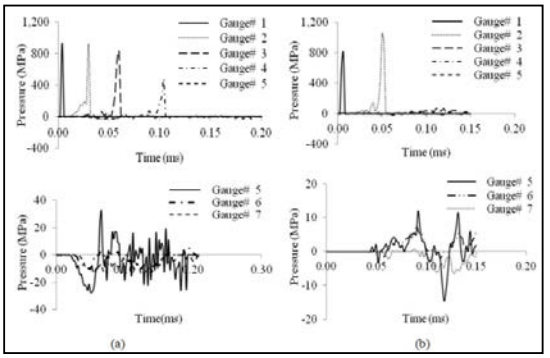

Fig. 4 Numerical responses of SSS type panel with 10% fibre thickness for 7.62 mm projectile (a) for 60 mm thick panels (b) for 100 mm thick panels

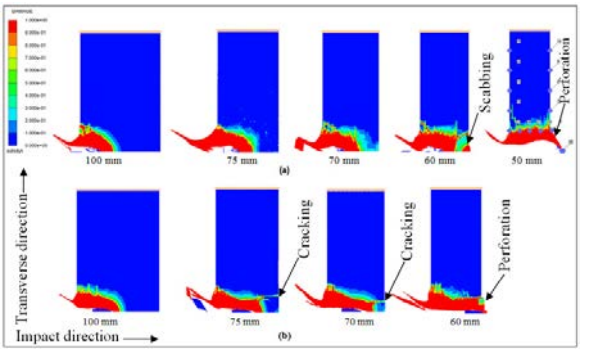

Fig.5 Damage contours for different thickness of panel with 10% fibre volume (a) Under 5.56 mm calibre projectile impact (b) Under 7.62 mm calibre projectile impact

4.6 Effect of Fibre Volume in SFRCC Panels

Keeping the thickness of the SSS type panels constant as 100 mm, the fibre volumes are varied to study its effect on impact resistance. The variations in DOP and crater diameter with respect to fibre content in 100 mm thick SFRCC (SSS) panels are shown in Fig. 6 for 7.62 mm calibre projectiles and similar trends were observed for 5.56 mm projectile. With the decrease in the fibre volume in composite panels, it is found that the cracking becomes severe due to impacts of both the projectiles.

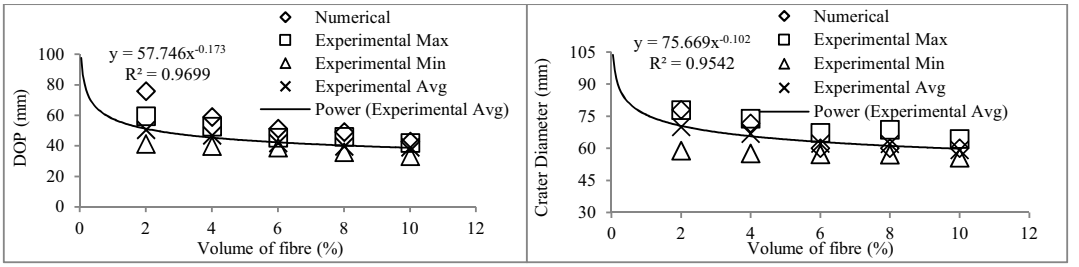

Fig.6 Comparison of numerical and experimental results for 7.62 mm projectile

5. Summary and Conclusions

The effect of thickness of panels, fibre volume on DOP and crater diameter are mainly investigated numerically and found to be compared well with experimental results. In order to reduce the computational complexities involved in 3D FE models, in this paper, a rather simplified axi-symmetric model is used in majority of the investigations

carried out. An appropriate material model (RHT model) for SFRCC is adopted with modified post peak behavior due to presence of fibres. The scabbing phenomenon was accurately predicted in SFRCC panels and validated the same through experimental investigations.The numerical results for fibre volume less than 4% found to deviate slightly, probably due to cracks in the panels. however for fibre volume more than 4% the numerical and experimental results corroborates well.RHT material model is found capable of model like, pressure hardening, strain hardening, strain rate hardening, third invariant dependence for compressive and tensile meridians, damage effects (strain softening), and crack-Softening.

Acknowledgements

The help rendered by the colleagues Dr. N. Anandavalli (Principal scientist) and Dr. J. Rajasankar (Chief scientist) of SVG, CSIR-SERC during experimental studies is highly acknowledged. This paper is being published with the kind permission of Director, CSIR-SERC, Chennai.

References

[1] Zukas J. A. (2004). Introduction to Hydrocodes, Studies in Applied Mechanics 49, Elsevier.
[2] Grote, D.L., Park, S.W., Zhou, M. (2001). Dynamic Behavior of Concrete at High Strain Rates and Pressures: I. Experimental Characterization. *Intl. Journal of Impact Engineering*, 25, 869-887.
[3] Naaman, A.E., Reinhardt H.W. and Fritz, C. (1992). Reinforced concrete beams with a SIFCON matrix. ACI Struct. J., 89, 79-88.
[4] Mougin, J.P., Perrotin, P., Mommessin, M., Tonnelo, J., andAgbossou, A. (2005). Rock Fall Impact on Reinforced Concrete Slab: An Experimental Approach. International *Journal of Impact Engineering*, 31, 169-183.
[5] Remennikov, A. and Kaewunruen, S. (2006). Impact resistance of reinforced concrete columns: experimental studies and design considerations. 19th Australasian Conference on the Mechanics of Structures and Materials, Nov 29 - Dec 1, Christchurch, New Zealand, 817-824.
[6] Thilakarathna, H.M.I., Thambiratnam, D.P., Dhandasekar, M., andPerera, N. (2010). "Numerical Simulation of Axially Loaded Concrete Columns under Transverse Impact and Vulnerability Assessment." International Journal of Impact Engineering, 37 (11) 1100-1112.
[7] Hagedorn, P. and DasGupta, A. (2007). *Vibrations and Waves in Continuous Mechanical Systems*, John Wiley and Sons, England.
[8] Clifton, J.R. (1982). Penetration Resistance of Concrete – A Review. National Bureau of Standards, Washington D.C., Special Publication 480-545.
[9] Anderson, W.F. Watson, A.J. and Kaminskyj, A.E. (1992). The resistance of SIFCON to high velocity impact. *Second Intl. Conference on Structures Under Shock and Impact*, 89-98.
[10] Zhang, X. X., Ruiz, G. and Yu, R. C. (2008). Experimental study of combined size and strain rate and size effects on the fracture of reinforced concrete. J. Mater. Civ. Eng., 20(8), 544-551.
[11] Borrvall, T. and Riedel, W. (2011). The RHT Concrete Model In LS-DYNA. *8th European LS-DYNA Users Conference,* Strasbourg.
[12] Fossum, A.F. and Brannon, R.M., (2004), The SANDIA GEOMODEL, Theory and users guide, Sandia national laboratories report SAND2004-3226, Albuquerque.
[13] Rebecca, M.B. and Seubpong, L. (2009). Survey of Four damage models for concrete. Sandia report, August.
[14] Nyström U., and GylltoftK.(2008). Comparative Numerical Studies of Projectile Impacts on Plain and Steel-Fibre Reinforced Concrete. Proceedings Nordic Concrete Research, Bålsta, Sweden*,* 198-199. ISBN/ISSN: 978-82-8208-007-1 Nr. 78252.
[15] Tu,Z. and Lu, Y. (2010). Modifications of RHT material model for improved numerical simulation of dynamic response of concrete. *Intl. Journal of Impact Engineering,*37, 1072-1082
[16] ACI Committee 544 (1982). State of the Art Report on Fiber Reinforced Concrete. *American Concrete Institute*, USA.
[17] Rempling R. (2004). Concrete wall subjected to fragment impacts-numerical analysis of perforation and scabbing, MS thesis, Chalmers University of technology, Sweden.
[18] Malvar, L.J., Crawford, J.E., Morrill, K.B. (2000). K&C Concrete Model Release III, Automated Generation of Material Model Input. Karagozian& Case Technical Report TR-99-24-B1. Glendale, Karagozian& Case Structural Engineers, 1-17.
[19] Riedel, W., Thoma, K., Hiermaier, S., Schmolinske, E. (1999). Penetration of reinforced concrete by BETA-B-500, Numerical analysis using a new macroscopic concrete model for hydrocodes, Proc. of 9th international symposium on interaction of the effects of munitions with structures, Berlin, 315-322.
[20] Zhang, M.H., Sharif, M.S.H., and Lu, G. (2007). Impact Resistance of High-Strength Fibre-Reinforced Concrete. Magazine of Concrete Research, 59, 199-209.
[21] AUTODYN (2011). Ansys Inc. AUTODYN Release Version 14.0. Southpointe, Canonsburg PA.
[22] CEB (1990), Comité Euro-International du Béton. CEB-FIP Model Code, Trowbridge, Wiltshire, UK: Redwood Books.
[23] Maalej, M., Quek S. T. and Zhang, J. (2005). Behaviour of Hybrid-Fifer Engineered Cementitious Composites Subjected to Dynamic Tensile Loading and Projectile Impact. *Journal of Materials in Civil Engineering*, 17, 143-152.
[24] Shah, A.A. and Ribakov, Y. (2011). Recent trends in steel fibred high-strength concrete. *Materials and Design,*32, 4122–4151.